AMERICAN SOCIETY FOR MICROBIOLOGY | Journal of Virology®

PATHOGENESIS AND IMMUNITY

Peripheral Blood Biomarkers of Disease Outcome in a Monkey Model of Rift Valley Fever Encephalitis

Elizabeth R. Wonderlich,[a,b]* Amy L. Caroline,[a,b] Cynthia M. McMillen,[a,b] Aaron W. Walters,[a] Douglas S. Reed,[a,c] Simon M. Barratt-Boyes,[a,b,c] Amy L. Hartman[a,b]

[a]Center for Vaccine Research, University of Pittsburgh, Pittsburgh, Pennsylvania, USA
[b]Department of Infectious Diseases and Microbiology, University of Pittsburgh, Pittsburgh, Pennsylvania, USA
[c]Department of Immunology, University of Pittsburgh, Pittsburgh, Pennsylvania, USA

ABSTRACT Rift Valley Fever (RVF) is an emerging arboviral disease of livestock and humans. Although the disease is caused by a mosquito-borne virus, humans are infected through contact with, or inhalation of, virus-laden particles from contaminated animal carcasses. Some individuals infected with RVF virus (RVFV) develop meningoencephalitis, resulting in morbidity and mortality. Little is known about the pathogenic mechanisms that lead to neurologic sequelae, and thus, animal models that represent human disease are needed. African green monkeys (AGM) exposed to aerosols containing RVFV develop a reproducibly lethal neurological disease that resembles human illness. To understand the disease process and identify biomarkers of lethality, two groups of 5 AGM were infected by inhalation with either a lethal or a sublethal dose of RVFV. Divergence between lethal and sublethal infections occurred as early as 2 days postinfection (dpi), at which point $CD8^+$ T cells from lethally infected AGM expressed activated caspase-3 and simultaneously failed to increase levels of major histocompatibility complex (MHC) class II molecules, in contrast to surviving animals. At 4 dpi, lethally infected animals failed to demonstrate proliferation of total $CD4^+$ and $CD8^+$ T cells, in contrast to survivors. These marked changes in peripheral blood cells occur much earlier than more-established indicators of severe RVF disease, such as granulocytosis and fever. In addition, an early proinflammatory (gamma interferon [IFN-γ], interleukin 6 [IL-6], IL-8, monocyte chemoattractant protein 1 [MCP-1]) and antiviral (IFN-α) response was seen in survivors, while very late cytokine expression was found in animals with lethal infections. By characterizing immunological markers of lethal disease, this study furthers our understanding of RVF pathogenesis and will allow the testing of therapeutics and vaccines in the AGM model.

IMPORTANCE Rift Valley Fever (RVF) is an important emerging viral disease for which we lack both an effective human vaccine and treatment. Encephalitis and neurological disease resulting from RVF lead to death or significant long-term disability for infected people. African green monkeys (AGM) develop lethal neurological disease when infected with RVF virus by inhalation. Here we report the similarities in disease course between infected AGM and humans. For the first time, we examine the peripheral immune response during the course of infection in AGM and show that there are very early differences in the immune response between animals that survive infection and those that succumb. We conclude that AGM are a novel and suitable monkey model for studying the neuropathogenesis of RVF and for testing vaccines and therapeutics against this emerging viral pathogen.

KEYWORDS African green monkey, Rift Valley fever virus, aerosols, bunyavirus, caspases, cytokines, encephalitis, viral pathogenesis

Received 19 September 2017 **Accepted** 1 November 2017

Accepted manuscript posted online 8 November 2017

Citation Wonderlich ER, Caroline AL, McMillen CM, Walters AW, Reed DS, Barratt-Boyes SM, Hartman AL. 2018. Peripheral blood biomarkers of disease outcome in a monkey model of Rift Valley fever encephalitis. J Virol 92:e01662-17. https://doi.org/10.1128/JVI.01662-17.

Editor Rebecca Ellis Dutch, University of Kentucky College of Medicine

Address correspondence to Amy L. Hartman, hartman2@pitt.edu.

* Present address: Elizabeth R. Wonderlich, Southern Research, Frederick, Maryland, USA.

Rift Valley fever (RVF) is an important emerging veterinary disease of livestock that is endemic throughout Africa. RVF causes widespread death of young ruminants and massive fetal loss in pregnant animals. Zoonotic spillover to humans occurs through mosquito bites or contact with infected animals. The World Health Organization (WHO) has repeatedly branded RVF as an important disease with the potential to cause a public health emergency due to insufficient vaccines and therapeutics (1). The risk of global spread (similar to that for Zika, Chikungunya, and West Nile viruses) is high due to the pervasive distribution of competent mosquito vectors throughout Europe and the Americas. The emergence of RVF in new locations, as demonstrated by its appearance in Saudi Arabia and Yemen in 2000, would cause considerable economic damage, in addition to fear and anxiety due to human morbidity and mortality (2–4).

RVF virus (RVFV) causes three distinct clinical diseases in humans: an acute nonlethal dengue-like febrile illness, severe hepatic/hemorrhagic disease, and meningoencephalitis (5–7). Either of the two severe forms of RVF occurs in 1 to 5% of naturally infected patients (5, 8, 9). Historically, RVF is most recognized for the hemorrhagic fever disease because of similarities in disease presentation to Ebola virus. However, neurological RVF occurs at about the same incidence as hemorrhagic RVF (7, 9). In South Africa in 1974–1975, 14% of patients with laboratory-confirmed cases developed encephalitis, compared to 6% who developed hemorrhagic fever (7). In Saudi Arabia in 2000, 17% of laboratory-confirmed patients reported central nervous system (CNS) symptoms, while 7% had hemorrhagic abnormalities (6). Of those with neurological disease, 53% died. In Tanzania in 2007, 89% of those whose deaths were confirmed had encephalopathy (8). Clinical symptoms of neurologic RVF in humans include severe headache, hallucination, disorientation, vertigo, excessive salivation, and weakness or partial paralysis (6, 7, 9, 10). Neurological RVF is clearly an important, yet overlooked and understudied, clinical outcome in humans, due primarily to the lack of an animal model that recapitulates neurological disease.

Although RVFV is mosquito borne, humans are frequently infected via mucosal exposure or inhalation of virus from contaminated animal carcasses (11–13). Retrospective studies have shown that severe RVF disease is associated with working as a herdsperson, handling sick animals, and slaughtering animals (7, 14–16). Whether the exposure route determines the clinical outcome is not fully known, but aerosol or intranasal exposure is more likely than percutaneous injection to result in encephalitis in lab animals (17–20) and potentially in humans (15).

In this report, we present an analysis of a novel nonhuman primate (NHP) model of RVF neurological disease. We sought to extend our previous observation that African green monkeys (AGM) (*Chlorocebus aethiops*) exposed to small-particle aerosols of RVFV develop neurological disease and succumb to infection (18). In the experiments reported here, we compared the metabolic and immune responses of AGM exposed to lethal or sublethal doses of the virulent RVFV strain ZH501. We obtained longitudinal blood samples from AGM during the course of infection in order to better understand the disease course and to identify biomarkers of lethality.

We report a dichotomy in the phenotype of peripheral blood T cells based on clinical outcome. Lethal infections were associated with the expression of T cell death markers, whereas surviving AGM displayed T cell activation markers and increased T cell numbers early after infection. In addition, we found a biphasic cytokine response associated with death or survival. Lethal infections were characterized by delayed antiviral cytokine production and late-onset serum inflammatory cytokine production; conversely, production of antiviral and proinflammatory cytokines in survivors occurred early and transiently. The direct relationship between changes in peripheral blood T cell populations and neurological disease is an area of intense continued interest. This study provides novel insight into the course of infection in RVFV-infected AGM, is a starting point for additional pathogenesis studies, and can be used as a basis for evaluating vaccines and therapeutics.

TABLE 1 Characteristics of animal cohort, aerosol infection, and outcome

Animal ID	Age (yr)	Wt (kg)	Exposure duration (min)	Min vol (ml/min)[a]	Presented (inhaled) dose (PFU)	Time to death (days)
132-13	9.9	5.2	20	900	2.9E+04	NA[e]
133-13	9.1	4.7	20	834	3.8E+04	NA
134-13	9.1	4.3	20	781	4.7E+05	NA
135-13	9.1	4.6	20	821	4.8E+05	NA
139-13	6.9	4.6	30	821	2.0E+05	NA
136-13	10.0	4.2	20	767	3.9E+05	10
137-13	7.2	4.2	30	767	9.3E+05	10
138-13	8.0	5.2	30	900	1.2E+06	9
140-13	8.9	6.1	30	1,015	1.4E+06	12
141-13	9.0	4.6	30	821	1.2E+06	11
Geometric mean for:						
Sublethal-infection group	8.8	4.7	22	831	1.4E+05	
Lethal-infection group	8.6	4.9	28	854	9.4E+05	10.4
P value	NS[b,c]	NS[c]	NS[d]	NS[c]	0.005[c]	

[a]Calculated using Guyton's formula.
[b]NS, not significant ($P > 0.05$).
[c]As determined by a *t* test.
[d]As determined by a Mann-Whitney test.
[e]Not applicable.

RESULTS

Clinical disease, LD_{50}, and fever in RVFV-infected AGM. In this study, two groups of 5 AGM were infected with lethal or sublethal doses of RVFV by inhalation. The lethal- and sublethal-infection groups did not differ in age, weight, exposure duration, or respiratory minute volume but differed in the inhaled (presented) dose (mean inhaled doses, 9.4×10^5 PFU and 1.4×10^5 PFU, respectively [Table 1; Fig. 1]). The dose range across all 10 animals was 50-fold. The 50% lethal dose (LD_{50}) calculated by probit analysis was 4.8×10^5 PFU, which is statistically indistinguishable from the LD_{50} of 1.7×10^5 PFU obtained from our previous study using a smaller cohort of 6 animals (18).

All AGM exhibited a decreased intake of food and water postexposure, and animals in both groups lost 5 to 10% of their body weight (Fig. 2). While the surviving animals recovered, the lethally infected AGM reached euthanasia criteria between 9 and 12 days postinfection (dpi). Several of the lethally infected AGM began drooling 24 to 36 h prior to euthanasia. Drooling was the first notable sign of neurological distress in these animals and has also been observed in human RVF (9). Within the last 24 h before euthanasia, most animals that succumbed displayed shivering, tremor, and/or stumbling off perch, which advanced quickly to an inactive, recumbent state, at which point the animals were euthanized. The only signs of illness that the surviving animals displayed were decreases in activity and food/water intake, resulting in weight loss during the 9- to 12-dpi period that rebounded upon recovery (Fig. 2).

Body temperature data were collected remotely using radiotelemetry. The actual and forecasted postexposure body temperature values are shown for one survivor, AGM 134-13 (Fig. 3A), and one lethally infected animal, AGM 136-13 (Fig. 3B). All of the lethally infected AGM developed substantial fevers beginning on days 6 to 7 dpi (range, 3.3 to 4.9°C above baseline [Fig. 3D and Table 2]). Three of the surviving animals developed notable fever (AGM 132-13, 133-13, and 134-13), and the other two surviving AGM developed only very mild changes in temperature (Fig. 3C; Table 2).

RVFV is shed from the respiratory tract after aerosol infection. In order to determine if inhalational exposure to RVFV results in shedding of the virus in respiratory tract secretions, nasal wash (NW) fluids were obtained from each animal every 2 days after infection. By use of plaque assays, infectious virus was detected transiently in the NW fluids of both groups at 2 dpi, with no statistical difference between the lethal- and

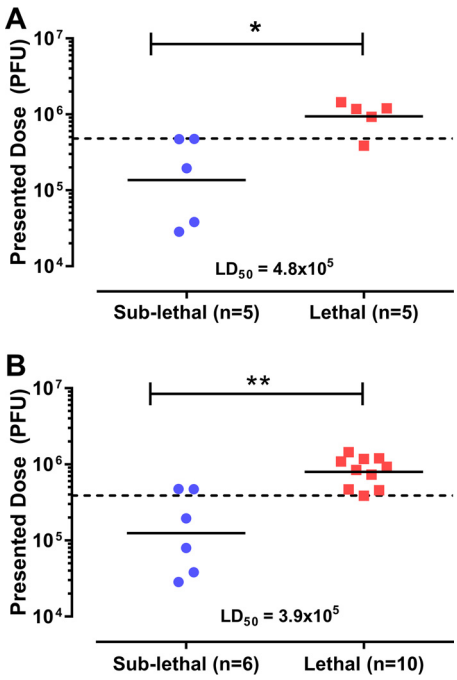

FIG 1 Comparison of inhaled doses of RVFV in African green monkeys by disease outcome. Shown is the inhaled (presented) dose (total PFU) received by each animal, stratified by clinical outcome. (A) Doses presented to the sublethal-infection ($n = 5$) and lethal-infection ($n = 5$) groups in this study. (B) Because the AGM from this study and our previous study (18) were infected using the same virus, methodology, and equipment, a combination of dosing data from both cohorts was used to calculate the overall LD_{50}. Asterisks indicate significance (*, $P < 0.05$; **, $P < 0.01$) by the Mann-Whitney test. For each group, a solid horizontal line indicates the geometric mean. The LD_{50} was calculated using probit analysis and is indicated by a dashed horizontal line.

sublethal-infection groups at this time point (Fig. 4A). In one lethally infected animal (AGM 136-13), infectious virus persisted in NW fluids through 6 dpi before becoming undetectable by 8 dpi. Reverse transcription-quantitative PCR (q-RT-PCR) analyses showed that viral RNA persisted longer than infectious virus. Viral RNA was present in NW fluids from all animals at all time points, and levels decreased through 8 dpi (Fig. 4B). Lethally infected animals tended to have higher levels of viral RNA than survivors, but there was no significant difference between the groups at any time point.

No infectious virus was detectable in plasma samples by plaque assays at any time after infection (data not shown). However, viral RNA was detected transiently in the plasma of all animals on days 2 and 4 postinfection, before trailing off to undetectable levels by 8 dpi (Fig. 4C). These data indicate that there was low-level transient peripheral viremia, and shedding of the virus through the nasal secretions is also possible. Virus levels in NW fluids and plasma had no clear association with disease outcome.

High levels of virus in the central nervous system are associated with lethal RVF disease. At the necropsy of each of the lethally infected animals, high levels of infectious virus were found throughout the brain and spinal cord, and low levels in the eye (Fig. 4D). Conversely, no infectious virus was found in the same tissues from the surviving animals. For both survival groups, no infectious virus was found in the lung, liver, spleen, kidney, or salivary glands. Only one animal (AGM 141-13) had detectable virus in the cerebrospinal fluid (CSF), even though all lethally infected animals had high levels of virus in the spinal cord. Animals from both groups showed evidence of viral RNA persisting in the brain, eye, spleen, liver, lung, and salivary gland by q-RT-PCR (Fig. 4E). This is remarkable given that the surviving animals were euthanized 28 dpi yet still had viral RNA levels similar to the lethally infected animals sacrificed 9 to 12 dpi. Since the 2 groups of animals were necropsied at different time points, statistical

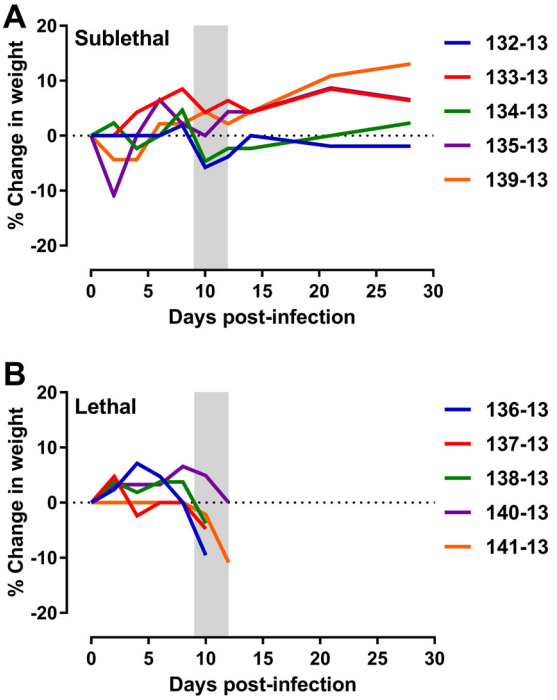

FIG 2 Weight loss in RVFV-infected AGM. Shown are the changes in body weight over time in the sublethal-infection (A) and lethal-infection (B) groups. On each graph, the shaded area represents the 9- to 12-day clinical window during which the lethally infected animals were euthanized due to severe disease.

comparison of the amount of viral RNA in the brain is not possible, but these data show that the surviving animals had virus present in the brain during infection despite not exhibiting noticeable clinical signs.

Granulocytosis and blood chemistry changes are a late feature of lethal infection. We noted previously that lethally infected AGM have significant changes in blood chemistry, such as total white blood cells (WBC), platelets, and blood urea nitrogen (BUN) in samples obtained at necropsy (18), but the timing of the onset of these changes was not determined. Here, complete blood counts (CBC), blood chemistry analysis, and flow cytometry were used to detect changes within the blood over the duration of infection. CBC indicated a significant increase in WBC late in the infection (10 to 12 dpi), consisting primarily of granuloctyes (GRA) in lethally infected AGM (Fig. 5A and B). Total WBC and GRA counts remained close to preinfection levels in surviving animals. There was a gradual increase in platelet numbers from 6 dpi onward in the survivors, while platelet levels did not change significantly over time in the lethally infected animals (Fig. 5C).

There were surprisingly few changes in blood chemistry between the two survival groups. Only BUN, amylase (AMY), and creatinine (CRE) were significantly elevated in the lethal-infection group at end-stage disease (10 to 12 dpi) (Fig. 5D to F). As we noted previously (18), liver damage is not a prominent feature of disease in aerosol RVFV-infected AGM, as evidenced by the fact that there were no major perturbations in alanine transferase (ALT) or alkaline phosphatase (ALP) levels (data not shown).

Expansion of T cells occurs early in surviving AGM but not in AGM with lethal infections. Using flow cytometry, we monitored changes in six different $CD45^+$ mononuclear peripheral blood cell populations over time (Fig. 6A), with groups stratified on the basis of clinical outcome. The absolute numbers of each cell type were compared to those in preinfection samples from the same animal and are expressed as percentages of preinfection levels. As early as 4 dpi and persistently throughout infection, the surviving monkeys had higher numbers of total $CD3^+$ T cells, comprising

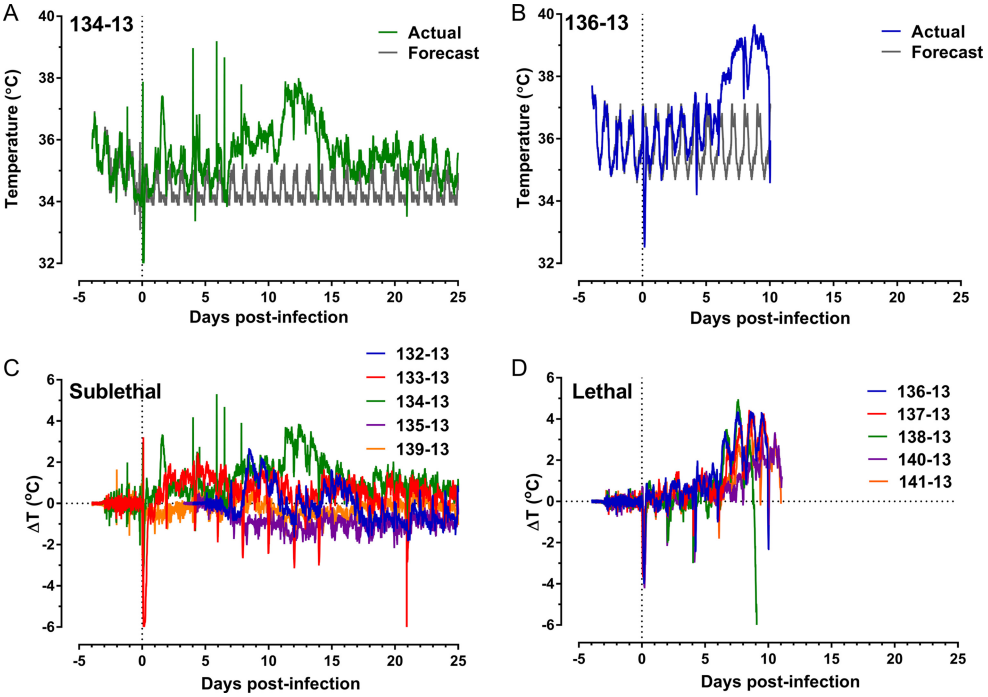

FIG 3 Febrile response in RVFV-infected AGM. (A and B) Actual body temperatures for M134-13 (A) and M136-13 (B) recorded every 15 min are superimposed on the predicted (forecast) normal diurnal body temperatures by use of ARIMA modeling. (C and D) Residual changes in body temperature were determined by subtracting the predicted temperature value from the actual temperature value recorded for each point and are expressed as changes in temperature [ΔT (°C)] for all surviving (C) and lethally infected (D) animals. In each graph, the vertical dashed line indicates the day of infection. For animals 132-13 and 135-13, some data points between −3 and 3 dpi are missing.

both $CD4^+$ and $CD8^+$ cells, in the peripheral blood (Fig. 6B to D), suggesting expansion of these two populations in survivors. The numbers of total $CD3^+$, $CD4^+$, and $CD8^+$ T cells in the blood of lethally infected AGM remained at preinfection levels. Conversely, lethally infected AGM had greater numbers of both monocytes and plasmacytoid

TABLE 2 Fever parameters in RVFV-infected AGM

Animal ID	Presented (inhaled) dose (PFU)	Time to death (days)	T_{max} (°C)[a]	R_{max} (°C)[b]	Duration (h)[c]	No. of fever hours[d]	Avg elev (°C)[e]
132-13[f]	2.9E+04		38.4	2.6	128.8	137.9	1.1
133-13	3.8E+04		38.2	3.2	41.0	70.1	1.7
134-13	4.7E+05		39.2	5.3	252.0	478.8	1.9
135-13[f]	4.8E+05		37.4	1.0	0.8	0.5	0.7
139-13	2.0E+05		37.1	1.1	5.5	4.3	0.8
136-13	3.9E+05	10	39.6	4.3	173.0	336.6	1.9
137-13	9.3E+05	10	39.3	4.4	153.5	277.1	1.8
138-13	1.2E+06	9	39.5	4.9	100.8	181.0	1.8
140-13	1.4E+06	12	38.6	3.3	131.5	184.3	1.4
141-13	1.2E+06	11	39.5	4.1	144.5	247.5	1.7
Geometric mean for:							
Sublethal-infection group	1.4E+05		38.1	2.6	85.6	138.3	1.2
Lethal-infection group	9.4E+05	10.4	39.3	4.2	140.7	245.3	1.7
P value[g]	0.005		0.017	0.097	NS	NS	0.096

[a]Maximum temperature during the course of infection.
[b]Maximum degree increase from the predicted value.
[c]Number of hours of significant temperature elevation.
[d]Sum of the hours of significant temperature elevation.
[e]Average temperature elevation during the febrile period.
[f]Missing data points between −3 and 3 dpi.
[g]Determined by the *t* test. NS, not significant ($P > 0.05$).

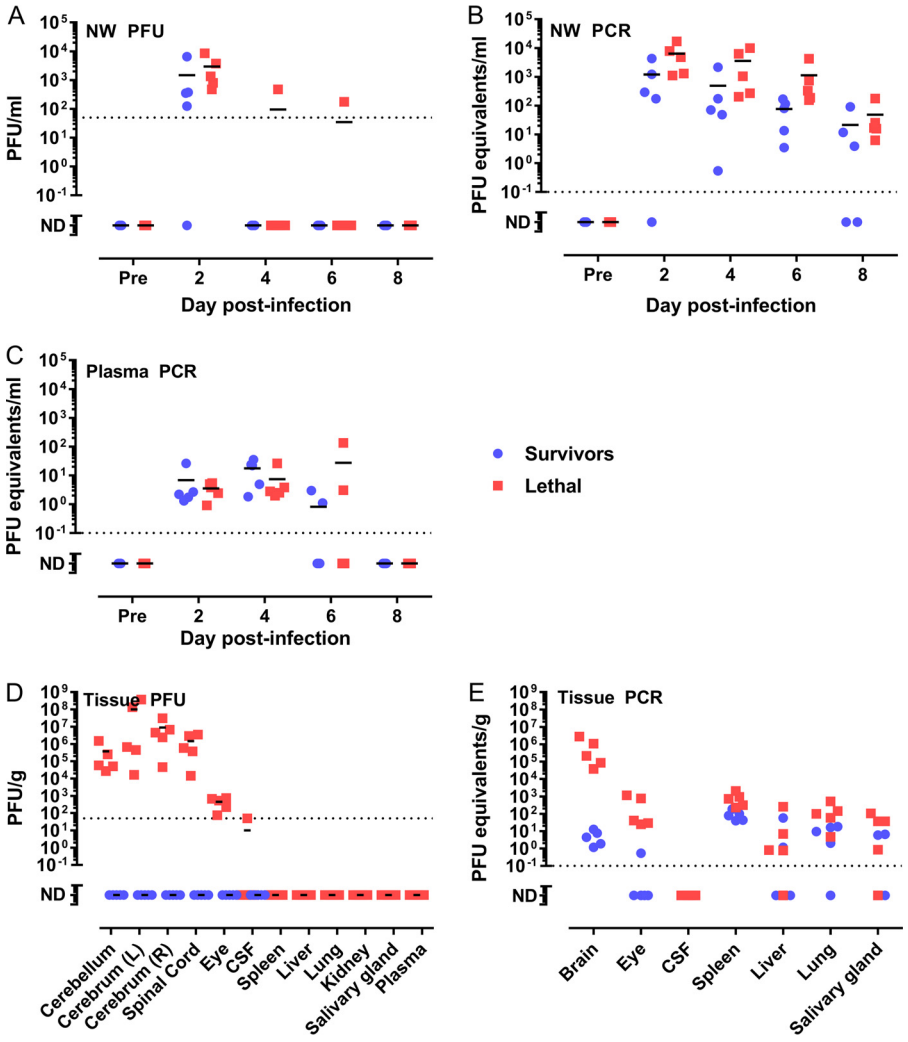

FIG 4 Virus detection in biological samples during RVFV infection of AGM. Levels of infectious virus in the sample types indicated were measured by a plaque assay (with results expressed as PFU per milliliter or per gram) or q-RT-PCR (with results expressed as PFU equivalents per milliliter or per gram). (A and B) Nasal wash; (C) plasma; (D and E) tissues. Dashed horizontal lines represent the limits of detection of the plaque assay (50 PFU) and PCR assay (0.1 PFU equivalent). ND, not detected (below the limit of detection); Pre, preinfection; L, left cerebrum; R, right cerebrum.

dendritic cells (pDC) later in infection (>8 dpi), whereas survivors had no changes from baseline (Fig. 6E and F). The numbers of myeloid dendritic cells (mDC) varied over the course of infection, but there were no significant differences between the groups (Fig. 6G).

Activation and death markers in T cell populations distinguish between surviving and nonsurviving AGM. To examine the phenotype of $CD4^+$ and $CD8^+$ cells in greater detail during acute RVFV infection, we measured activation, proliferation, and apoptosis through flow cytometry. As an indicator of T cell activation, analysis of the mean fluorescence intensity (MFI) of major histocompatibility complex class II (MHC-II) molecules revealed that both $CD4^+$ and $CD8^+$ T cells exhibited an increase in MHC-II expression at 2 dpi in surviving AGM (Fig. 7A and B), which is 2 days prior to an increase in the total cell numbers on 4 dpi (Fig. 6C and D). This increase was transient in the $CD4^+$ T cell population but remained 50% above preinfection levels in $CD8^+$ cells from surviving AGM. Within the lethally infected AGM group, MHC-II expression on $CD4^+$ or $CD8^+$ cells remained at baseline levels. Cell proliferation measured by Ki-67 revealed that there were no major differences in this proliferation marker within either cell type between the two survival groups (data not shown).

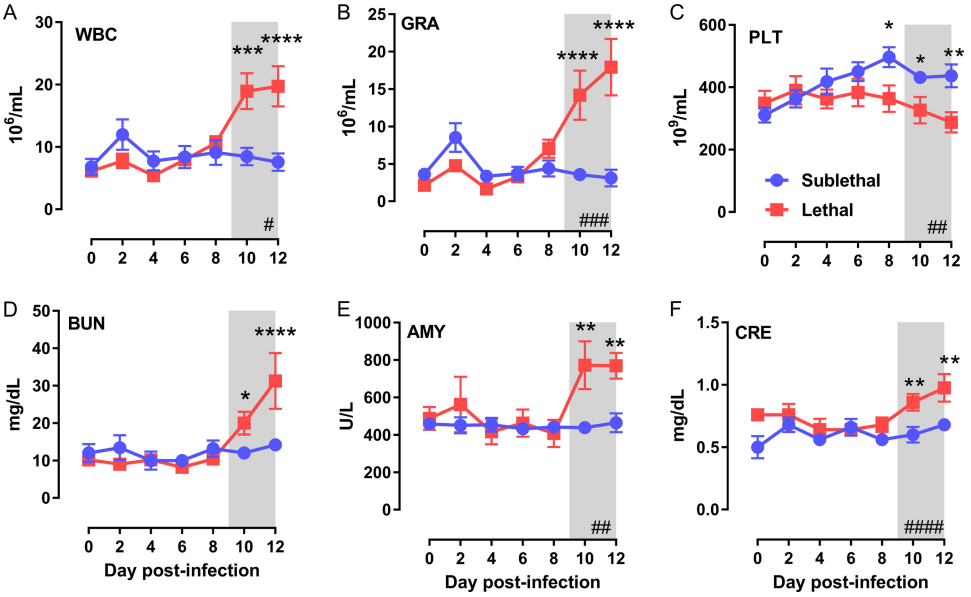

FIG 5 Granulocytosis and blood chemistry changes are a late feature of lethal infection. Blood collected every 2 days was used for CBC with 3-part differential analysis and a 14-parameter blood chemistry panel. (A) Total white blood cells (WBC); (B) granulocytes (GRA); (C) platelets (PLT); (D) blood urea nitrogen (BUN); (E) amylase (AMY); (F) creatinine (CRE). Hashtag symbols in the lower right corner indicate that time is a significant variable as determined by 2-way ANOVA (#, $P < 0.05$; ##, $P < 0.01$; ###, $P < 0.001$; ####, $P < 0.0001$). Multiple-comparison tests were performed at each time point, and asterisks above symbols indicate significant differences at a particular time point (*, $P < 0.05$; **, $P < 0.01$; ***, $P < 0.001$; ****, $P < 0.0001$). Shaded areas represent the 9- to 12-day clinical window.

Caspase-3 is a central player in the intrinsic and extrinsic apoptosis pathways. Analysis of the enzymatically active form of caspase-3 within $CD8^+$ T cells revealed a 10-fold increase in the number of cells expressing active caspase-3 in lethally infected animals over preinfection levels and levels in surviving animals (Fig. 7D). This increase began as early as 2 dpi and persisted throughout infection. This is the same time (2 dpi) at which the surviving monkeys are increasing the expression of MHC-II molecules on $CD8^+$ T cells (Fig. 7B). In $CD4^+$ cells, lethally infected AGM expressed more active caspase-3 on the day of necropsy than the surviving AGM. No significant changes in MHC-II, Ki-67, or active caspase 3 were seen in any of the other cell populations examined (mDC, pDC, monocytes [data not shown]).

Biphasic inflammatory cytokine responses. In addition to changes in the phenotype of leukocyte populations, we compared the cytokine and chemokine responses to RVFV in survivors and nonsurvivors. Cytokines and chemokines were measured over time in serum samples as well as in necropsy brain tissue samples using a 13-analyte multiplex assay. In agreement with flow cytometric data revealing an immune response early in infection, the survivors had a higher inflammatory response in the serum at 2 to 6 dpi, comprising interleukin 8 (IL-8), monocyte chemoattractant protein 1 (MCP-1), IL-6, soluble CD40 ligand (sCD40L), IL-10, and IL-1RA (Fig. 8A to D and 9A). In a separate assay, we measured serum alpha interferon (IFN-α) levels and found significantly higher levels in the serum of surviving animals at 2 dpi, which coincides with MHC class II induction (Fig. 8G). In contrast, lethally infected AGM had late increases (10 to 12 dpi) in the markers granulocyte colony-stimulating factor (G-CSF), sCD40L, IFN-γ, IL-10, IL-13, IL-18, IL-2, MIP-1β, transforming growth factor α (TGF-α), and tumor necrosis factor alpha (TNF-α) (Fig. 8D and E and 9B).

Multiplex assays were also run using brain samples from lethally infected AGM (necropsied 9 to 12 dpi) and convalescent survivors (necropsied 28 dpi). Very high levels of the inflammatory cytokines G-CSF, IFN-γ, IL-10, IL-18, IL-1α, IL-1Ra, IL-6, IL-8, and MCP-1 were found within the brains of lethally infected animals (Fig. 9C). A direct comparison cannot be made with the cytokines and chemokines found in the brains of

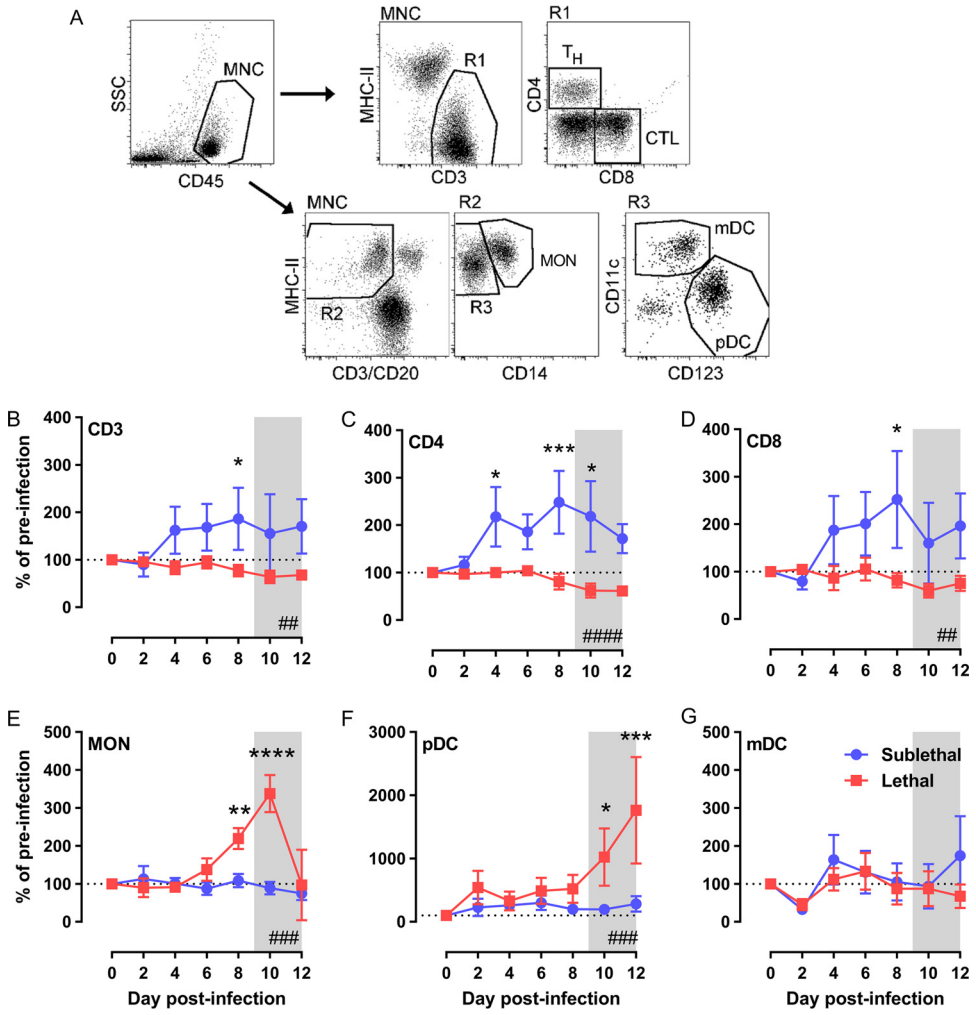

FIG 6 Expansion of T cells occurs early in surviving AGM but not in AGM with lethal infections. (A) Flow cytometry gating strategy used to identify the six cell populations indicated. $CD45^+$ mononuclear cells (MNC) were further separated into $CD3^+$ cells (R1) and then into $CD4^+$ (T_H) and $CD8^+$ (CTL) cells. The non-T- and non-B-cell MHC class II-positive MNC (R2) were further separated into $CD14^+$ monocytes (MON) and $CD14^-$ (R3) mDC ($CD11c^+$) and pDC ($CD123^+$). (B through G) The absolute numbers of each cell type are expressed as percentages of preinfection levels. (B) Total $CD3^+$ cells; (C) $CD4^+$ cells; (D) $CD8^+$ cells; (E) monocytes; (F) pDC; (G) mDC. Hashtag symbols in the lower right corner indicate that time is a significant variable as determined by 2-way ANOVA (#, $P < 0.05$; ##, $P < 0.01$; ###, $P < 0.001$; ####, $P < 0.0001$). Asterisks above symbols indicate significant differences at a particular time point (*, $P < 0.05$; **, $P < 0.01$; ***, $P < 0.001$; ****, $P < 0.0001$) as determined by multiple-comparison tests. Shaded areas represent the 9- to 12-day clinical window.

surviving AGM because these samples and the samples from lethally infected AGM were obtained at different points after infection.

Despite the differences we noted here regarding T cells and cytokines, all AGM developed virus-specific total IgG (measured by an enzyme-linked immunosorbent assay [ELISA]) and neutralizing antibodies (measured by 80% plaque reduction neutralization titers [$PRNT_{80}$]), including the two surviving animals that had mild febrile responses (data not shown).

DISCUSSION

Early experimental infection of monkeys with RVFV revealed that most species develop asymptomatic or mild disease (13, 21, 22). Among rhesus macaques, 20% of the animals infected intravenously (i.v.) developed severe disease resembling hemorrhagic fever (23, 24). These animals had prolonged clotting times, rash, and extensive necrosis of the liver (25). The rhesus model has been used in a limited number of

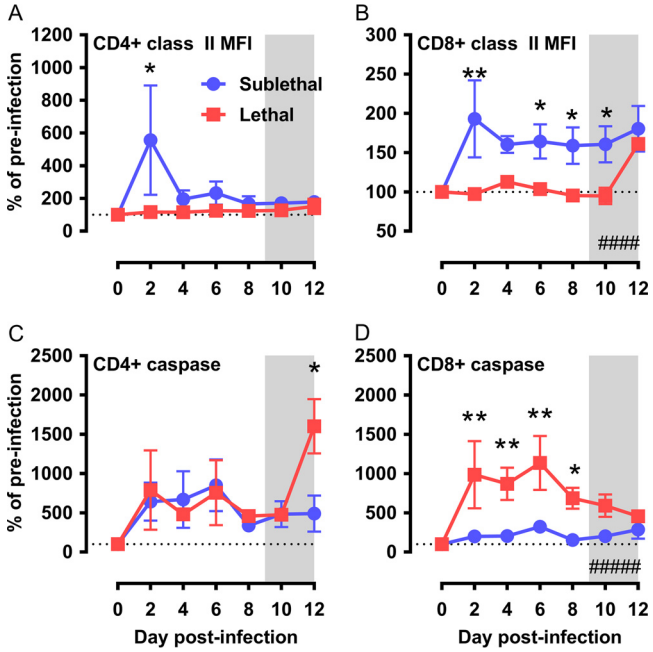

FIG 7 Activation and death markers in T cell populations distinguish between surviving and nonsurviving AGM. Using the gating strategy shown in Fig. 6A, $CD4^+$ and $CD8^+$ T cells were further characterized by expression of MHC class II molecules and active caspase-3. (A and B) Mean fluorescence intensity (MFI) of MHC class II expression on $CD4^+$ (A) and $CD8^+$ (B) T cells. (C and D) $CD4^+$ (C) and $CD8^+$ (D) T cells expressing active caspase-3. Hashtag symbols in the lower right corner indicate that time is a significant variable as determined by 2-way ANOVA (#, $P < 0.05$; ##, $P < 0.01$; ###, $P < 0.001$; ####, $P < 0.0001$). Asterisks above symbols indicate significant differences at a particular time point (*, $P < 0.05$; **, $P < 0.01$; ***, $P < 0.001$; ****, $P < 0.0001$) as determined by multiple-comparison tests. Shaded areas represent the 9- to 12-day clinical window.

experimental vaccine trials (26–28); however, the fact that severe or lethal disease is seen only in 20% of infections and the group size limitations of monkey studies make the interpretation of vaccine efficacy data challenging.

Previously, four species of monkeys were exposed to small-particle aerosols of RVFV (18). Rhesus and cynomolgus macaques developed a nonlethal febrile disease, while AGM and marmosets both developed lethal encephalitis. The susceptibility of AGM to lethal neurological disease was surprising given that other African monkey species tested in the past had been resistant (21). AGM (also known as vervet monkeys) do not appear to be a reservoir or natural host of RVFV in the wild, since screening of sera from AGM from the Rift Valley of Kenya did not yield positive results (29). The larger size of AGM than of marmosets (4 to 6 kg compared to 200 to 300 g, respectively) makes AGM more suitable for longitudinal natural history studies that require multiple blood samples. Also, considering the successful use of AGM for the evaluation of therapeutics against other viruses and bacteria (30–34), we chose to use AGM for the longitudinal study presented here.

Clinical symptoms of neurologic RVF in humans span a spectrum from acute to chronic, with common symptoms including meningeal irritation (as defined by neck stiffness, photophobia, and headache), confusion, delirium, hallucination, disorientation, vertigo, excessive salivation, teeth grinding, and weakness or partial paralysis (6, 7, 9, 10). Several of the AGM infected here developed hypersalivation as one of the first indications of neurological distress. We did not note any paralysis; however, the animals had tremors and frequently had trouble remaining upright on the perch within the cage. This may have been an outward manifestation of disorientation or vertigo.

Due to the aerosol exposure route, and because RVFV can be shed from the nasopharyngeal washings of humans (35), we looked for infectious virus in NW fluids. We found transient shedding of infectious virus and persistence of viral RNA in both

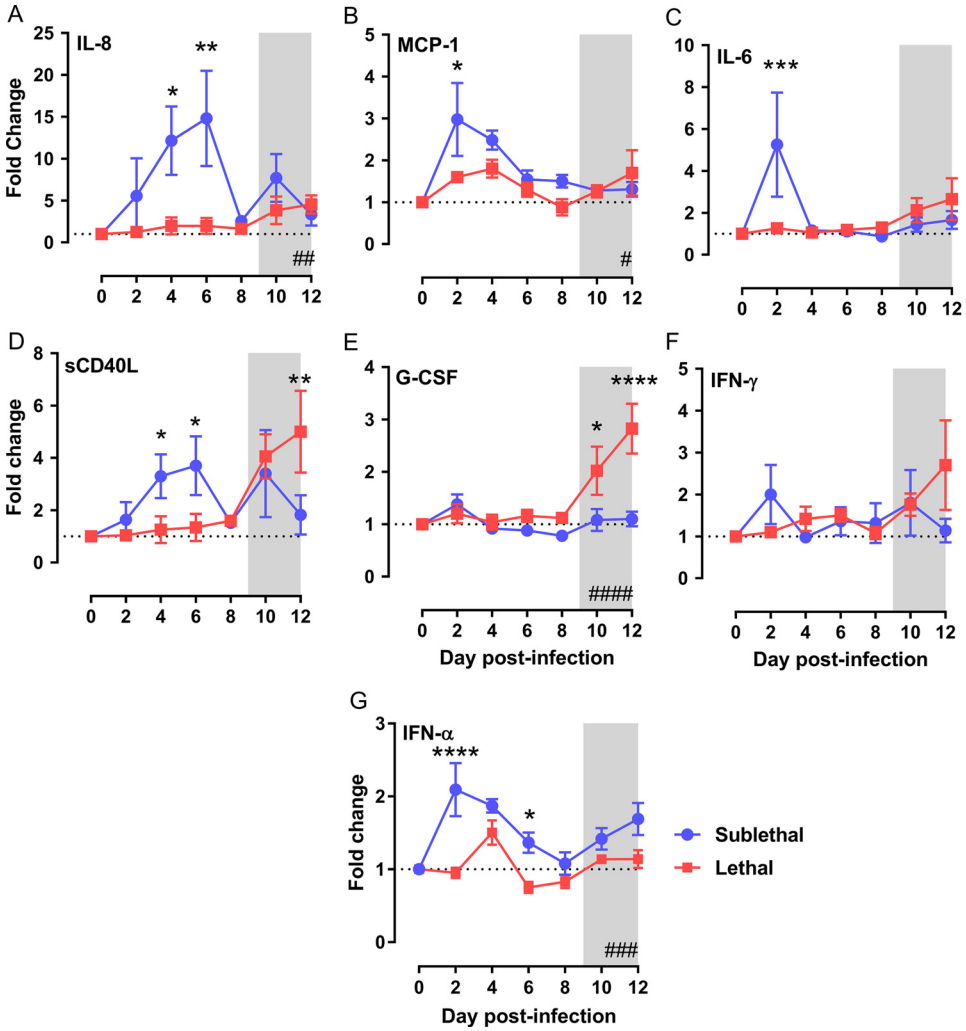

FIG 8 Early production of inflammatory cytokines in surviving RVFV-infected AGM. The fold change over preinfection levels is shown along the *y* axis. (A through F) Cytokines were measured by a 23-parameter monkey-specific magnetic bead multiplex assay. (A) IL-8; (B) MCP-1; (C) IL-6; (D) sCD40L; (E) G-CSF; (F) IFN-γ. (G) IFN-α was measured by ELISA. Hashtag symbols in the lower right corner indicate that time is a significant variable as determined by 2-way ANOVA (#, $P < 0.05$; ##, $P < 0.01$; ###, $P < 0.001$; ####, $P < 0.0001$). Asterisks above symbols indicate significant differences at a particular time point (*, $P < 0.05$; **, $P < 0.01$; ***, $P < 0.001$; ****, $P < 0.0001$) as determined by multiple-comparison tests. Shaded areas represent the 9- to 12-day clinical window.

outcome groups. The amount of virus secreted in NW fluids was not an indicator of the severity of infection or clinical outcome, and the possibility of transmission from this level of virus in respiratory secretions is unknown, but such transmission is theoretically possible. In contrast to NW fluids, we were not able to detect infectious virus in the plasma but were able to detect transient low levels of viral RNA by PCR, indicating that transmission via blood is less likely than transmission via respiratory secretions.

At end-stage disease in lethally infected AGM, infectious virus was concentrated in CNS tissues, with no live virus detectable in the peripheral tissues, such as liver and spleen, even in these very sick animals. This is consistent with the neurological clinical signs in the animals, as well as with the fact that liver and kidney damage was not a prominent feature of the disease course based on blood chemistry analysis. Viral RNA was found at low levels in the livers, spleens, and lungs of all animals, including survivors, suggesting that the virus does replicate in these tissues early in the course of infection, but infectious particles are no longer detectable by the time of death in either survivors or nonsurvivors. Surprisingly, surviving animals also had viral RNA in brain tissues even 28 days after infection. The virus is therefore able to reach the brain in the

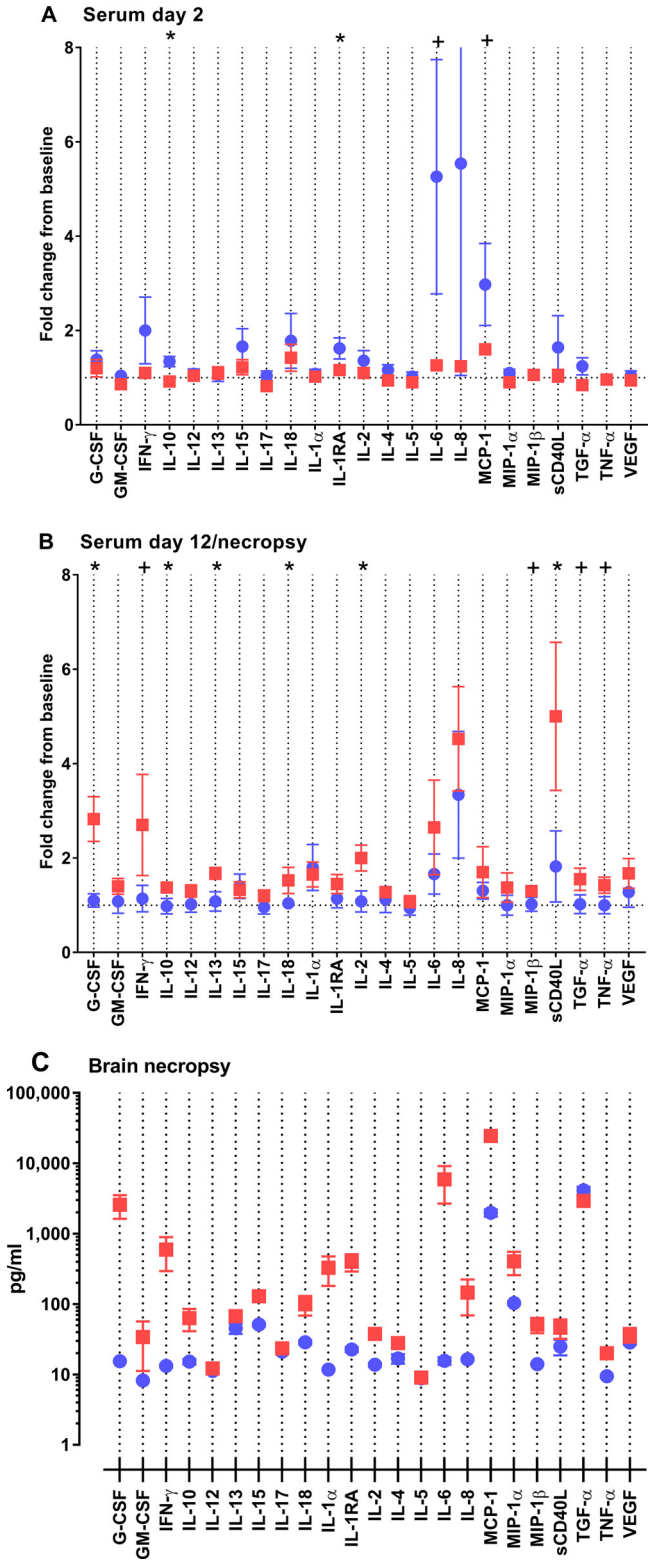

FIG 9 Early and late cytokine responses to RVFV infection differ between surviving and nonsurviving AGM. Serum and homogenized brain samples were analyzed using the 23-plex magnetic bead assay. (A and B) Results for serum samples at 2 dpi (A) and at necropsy (for the lethal infections) or 12 dpi (for the survivors) (B) are shown as the fold change over preinfection levels. Results of *t* tests are indicated by asterisks ($P < 0.05$) and plus signs ($0.05 < P < 0.1$). (C) Brain samples obtained at necropsy; levels of analytes are expressed in picograms per milliliter (*y* axis).

TABLE 3 Biomarkers indicative of lethal disease in RVFV-infected AGM

Biomarker	Time point (dpi)
Increased active caspase-3 expression in $CD8^+$ T cells	2
Lack of class II induction on $CD8^+$ T cells	2
Delayed serum IFN-α production	2
Lack of increase in absolute no. of total $CD4^+$ and $CD8^+$ cells	4
Peak febrile response	7–9
Increased no. of WBC	10
Increased no. of granulocytes	10

surviving animals but remains controlled, in contrast to uncontrolled replication in lethal infections. The mechanism behind the control of virus replication in the brain or the lack thereof in lethal infections warrants further investigation. Viral RNA found in the survivors' brains was not associated with infectious virus by plaque assay. Given the discovery that Ebola virus can persist in immune-privileged sites such as the brain and potentially reactivate in humans and monkeys (36, 37), it is interesting to speculate whether the virus would recur in surviving AGM if they were allowed to progress for additional months or were subjected to an immunosuppressive event.

Granulocytosis, thrombocytopenia, and elevated BUN and CRE levels are common characteristics of severe disease caused by RVFV and other pathogenic viruses, such as Ebola virus and Crimean-Congo hemorrhagic fever (CCHF) virus (38–40). Serum samples from 26 patients from the 2000 outbreak of RVFV in Saudi Arabia showed increased WBC and decreased platelets in fatal cases relative to levels in survivors (6, 41). Elevated CRE and urea levels were found in patient samples from lethal cases from the 2010 South African outbreak of RVFV (42). Granulocytosis has also been noted in NHPs exposed to aerosolized encephalitic alphaviruses, particularly in severe or fatal infections (43–46), as well as in human Japanese encephalitis cases (47, 48). In fact, human case reports for generalized viral encephalitis point toward significant neutrophilia in the blood and brain (49). This suggests that there are likely common pathogenic mechanisms of viral encephalitides that merit further study.

Few studies of RVF infection in NHPs have investigated peripheral blood lymphocyte changes in any depth. Immunological analyses in previous NHP studies were limited to the detection of neutralizing antibodies or total virus-specific IgG (19, 23, 24); however, our study found that these parameters did not correlate with survival or lethal disease. Instead, we found that total numbers of both $CD4^+$ and $CD8^+$ T cells increased in the peripheral blood of surviving monkeys but not in those that succumbed to infection. In confirmation of this notion, $CD4^+$ and $CD8^+$ T cells from surviving AGM had increased expression levels of MHC class II molecules, whereas increased expression of the apoptosis enzyme active caspase 3 occurred within the $CD8^+$ cells of lethally infected AGM (Table 3). The MHC-II induction and increase in cell numbers in the surviving animals suggests that they are able to mount an appropriate response and proliferate. The lack of increase in MHC-II levels and in apoptosis markers in lethally infected animals suggests that their cellular response is inadequate. In mice, an ineffective or delayed systemic immune response is associated with lethal RVF encephalitis (50–52).

Despite the clear differences we found in peripheral blood T cells, the two groups of AGM developed similar levels of total virus-specific IgG and neutralizing antibodies. This is in contrast to some reports on mice where lethal encephalitis is associated with a delayed humoral immune response, although those studies used a mutant virus deleted for the NSs protein (50, 53). While we were not able to examine virus-specific T cells in this study, previous studies using mice suggest that nonneutralizing epitopes within the RVFV nucleoprotein (N) elicit strong and potentially protective $CD8^+$ T cell responses that are more effective than neutralizing antibodies against the glycoprotein (GP) (52, 54, 55). Collectively, these data suggest that the innate and cellular immune responses may be more important than neutralizing antibodies for protection from lethal neurological RVF.

Macrophages are permissive to *in vitro* infection with RVFV (41) and are thought to

be an important early target for the virus *in vivo*. For RVFV, Ebola virus, CCHF virus, and other highly pathogenic viruses, the pattern of cytokine secretion in serum can portend survival, while an uncontrolled inflammatory response is associated with increased fatality (40–42, 56, 57). In this study, longitudinal analysis of cytokines in the serum suggests a biphasic pattern during encephalitic RVFV infection of AGM. Early in infection, surviving AGM had higher levels of antiviral and proinflammatory cytokines, such as IFN-α, IFN-γ, IL-6, IL-8, and MCP-1, while lethally infected animals had cytokine levels similar to those in the preinfection period. We hypothesize that the production of these mediators early after infection is a sign of immune response induction in animals that survive. Early antiviral and proinflammatory gene expression has been associated with resistance to severe disease in mouse models of RVFV (58). Conversely, late in infection, lethally infected AGM had elevated serum inflammatory cytokine levels and elevated numbers of both monocytes and pDC populations in the peripheral blood. The production of G-CSF, sCD40L, IL-8, IFN-γ, and IL-2 late in infection likely comes too late to help the host and is possibly indicative of a pathogenic cytokine storm that may contribute to the adverse outcome. Despite the elevated numbers of monocytes and pDC late in infection, lethally infected animals did not have more IFN-α in serum at this time.

High levels of inflammatory cytokines were found in the brain tissues of lethally infected animals at the time of euthanasia. Although we have only a single time point at which to examine tissue-level cytokine production, this massive inflammatory response appears to be pathological. In longitudinal serial sacrifice experiments performed in rat and mouse models of RVFV encephalitis, high proinflammatory cytokines are found in the brain at end-stage disease but not earlier (20, 50).

The most likely explanation for our findings hinges on the dose that each animal received. We hypothesize that in lethal infections, early proinflammatory cytokine production and induction of an antiviral state are dampened, possibly due to the effectiveness of the viral NSs protein at counteracting these host processes (59–61). Evidence for this is provided by the delayed and dampened induction of IFN-α in serum relative to that in surviving animals. Overall, this leads to poor induction of T cell immunity, as evidenced by the lack of T cell expansion, the expression of apoptotic markers in T cells, and the late cytokine storm in the serum and brain tissue. Conversely, early in infection in surviving animals, the secretion of proinflammatory (IFN-γ, IL-6, IL-8, MCP-1) and antiviral (IFN-α) mediators helps to curb early virus replication and also initiates an effective cellular immune response. The serum cytokine levels in survivors late in infection are closer to preinfection levels. It is likely that the lower challenge dose that the surviving animals received allowed them to overcome NSs-mediated effects and to mount a more-effective antiviral and innate immune response than the lethal animals receiving a higher dose.

Underlying individual genetic variation may also contribute to survival or death after infection (15, 62). Genetic polymorphisms in innate immune pathways are increasingly recognized for their role in determining the severity of RVFV infections in humans and lab animals (58, 62, 63). Small nucleotide polymorphism (SNP) analysis of human case samples from Kenya showed that SNPs in Toll-like receptor 3 (TLR3), TLR7, TLR8, myeloid differentiation primary response 88 (MyD88), TIR domain-containing adaptor inducing IFN-β (TRIF), mitochondrial antiviral-signaling protein (MAVS), and retinoic acid-inducible gene 1 protein (RIG-I) are associated with severe disease. In particular, the TLR3-TRIF pathway, as well as SNPs in IL-6, TLR-8, TRIF, and C-C chemokine receptor type 5 (CCR5), were all associated with severe meningoencephalitis (62).

In conclusion, we demonstrated that there are distinct differences in peripheral blood leukocyte populations and soluble mediators both early and late in infection that correspond with clinical outcome in RVFV-infected AGM. Our ongoing studies continue to investigate the relationship between the virus-specific immune response in the peripheral blood and the ability to control virus replication in the brain. We have shown that AGM develop a disease that has reproducible clinical signs and laboratory findings similar to what is seen in humans with neurological RVF disease. AGM are therefore a

relevant model with which to study the pathogenesis of neurological RVF, which could lead to the development of new treatments for this often-overlooked clinical outcome. The similarity of neurological RVF in AGM to what has been reported in other acute arboviral encephalitides in animals or humans suggests that lessons learned from neurological RVF could be broadly applicable to other encephalitic infections.

MATERIALS AND METHODS

Ethics, approvals, and oversight. All animal studies performed for this study and reported here adhered to the *Guide for the Care and Use of Laboratory Animals* of the National Institutes of Health (NIH) (64) and the Animal Welfare Act (AWA). Animal studies adhered to the principles stated in the Public Health Services Policy on Humane Care and Use of Laboratory Animals. Additionally, all animal protocols were approved and overseen by the University of Pittsburgh Institutional Animal Care and Use Committee (IACUC) and the Department of the Army's Animal Care and Use Review Office (U.S. Army Medical Research and Materiel Command [USAMRMC]). The University of Pittsburgh is fully accredited by the Association for Assessment and Accreditation of Laboratory Animal Care (AAALAC).

Biosafety information. The University of Pittsburgh Regional Biocontainment Laboratory (RBL) is a registered entity with the Federal Select Agent Program (FSAP) for work with Rift Valley fever virus. All work with infectious RVFV was conducted at biosafety level 3 (BSL-3)/animal biosafety level 3 (ABSL-3). The RBL is a shower-out facility, requiring a full clothing change into dedicated scrubs upon entry and a personal shower upon exit. All personnel wore powered air-purifying respirators (Versaflo TR-300; 3M, St. Paul, MN) when handling infectious samples or working with animals. A class III biological safety cabinet (BSC) was used for aerosol exposure of the animals. Vesphene IIse detergent (dilution, 1:128; Steris Corporation, Erie, PA) was used to disinfect all liquid wastes and surfaces. Solid wastes, caging, and animal wastes were steam sterilized.

Virus. RVFV (strain ZH501) was obtained from B. Miller (CDC, Fort Collins, CO) and S. Nichol (CDC, Atlanta, GA). Prior to receipt, the virus was generated from reverse genetics plasmids containing the wild-type ZH501 sequence, which was confirmed by sequencing. The virus used in this study was propagated using confluent Vero E6 cells (ATCC), and the titer was determined using a viral plaque assay, as described previously (17). For aerosol infections, the virus stock was diluted to the desired concentration in Dulbecco's modified Eagle medium (DMEM) containing 2% fetal bovine serum (FBS), penicillin-streptomycin, 10 mM HEPES buffer, 0.1% antifoam-Y emulsifier, and 0.1% glycerol.

Animals. Ten female adult African green monkeys (AGM) (*Chlorocebus aethiops*) were obtained from the Wake Forest Primate Center. AGM were housed in ABSL-2 facilities at the University of Pittsburgh for quarantine and prior to entrance into this study. Each animal used in this study was surgically implanted with a telemetry device placed subcutaneously between the scapulae (TA-D70 implant; Data Sciences International, St. Paul, MN) to monitor body temperature and activity. After a 2-week recovery period, the animals were transferred to the RBL ABSL-3 facility for the duration of these studies.

Aerosol exposures. AGM were infected via inhalational exposure was conducted using the AeroMP exposure system (Biaera Technologies, Hagerstown, MD) inside a class III BSC (Baker, Sanford, ME). AGM were anesthetized by intramuscular (i.m.) injection of tiletamine-zolazepam (6 mg/kg of body weight) or ketamine (9 mg/kg). Once anesthesia was confirmed, lung capacity was measured using plethysmography (Buxco Research Systems, Wilmington, NC) immediately prior to aerosol exposure. AGM were then transported to the class III BSC and were exposed to aerosols containing RVFV within a head-only exposure chamber (Biaera Technologies, Hagerstown, MD). A 3-jet collison nebulizer (BGI, Inc., Waltham, MA) was used to generate the aerosols, and aerosol samples were collected in an all-glass impinger (AGI; Ace Glass, Vineland, NJ). The amount of virus in the nebulizer and AGI was measured by a standard viral plaque assay, and the presented dose for each animal was calculated as described previously (65, 66). For this study, the 10 AGM were infected in 2 groups of 5 animals. AGM were monitored and scored on a set of criteria that included body temperature, weight, food and water intake, appearance, and behavior. Animals that reached the designated score threshold or were either comatose or moribund were euthanized promptly by intravenous (i.v.) injection of sodium pentobarbital; once death was verified, a necropsy was performed on each animal, and tissue samples were collected for histological and virological analyses.

Radiotelemetry. Baseline telemetry data were collected for 3 to 5 days before exposure to RVFV and for the entire duration of the study after infection. Body temperature was recorded every 15 min using the DataQuest A.R.T. 4.0 system (Data Sciences International). Analyses of telemetry data were conducted as described previously (18). Briefly, data collected before exposure were used to forecast predicted postexposure values using an autoregressive integrated moving average (ARIMA) model in NCSS software (Number Cruncher Statistical Systems, Kaysville, UT). Residual changes were determined by subtracting the predicted value from the actual value recorded for each point. Residual changes greater than 3 standard deviations were used to compute R_{max} (maximum increase over the predicted value), fever duration (number of hours of significant temperature elevation), and fever hours (sum of the significant temperature elevations).

Sample collection and processing. Saphenous-vein blood sampling was performed every other day for the first 2 weeks after infection; then weekly blood draws were performed until elective sacrifice at 28 days postinfection. At the same time as the blood draws, nasal swabs were obtained using the universal viral transport system (BD Biosciences). Blood collected into lithium-heparin-containing tubes was used for measurement of blood chemistry parameters with a VetScan VS2 analyzer (Abaxis, Union City, CA). Blood collected into K_2-EDTA-containing tubes was used for CBC analysis (VetScan HM2

analyzer; Abaxis), plasma collection, and peripheral blood mononuclear cell (PBMC) processing by layering under lymphocyte separation medium (LSM; catalog no. 0850494; MP Bioscience). Absolute blood counts were determined using Trucount tubes (BD Biosciences, Santa Ana, CA) as described previously (67). Cytokines were measured in plasma using a Milliplex MAP Non-Human Primate Cytokine magnetic bead panel (23-plex; EMD Millipore, Billerica, MA). IFN-α was measured in serum samples using the VeriKine monkey-specific IFN-α ELISA kit (PBL Assay Science, Piscataway, NJ). Tissue specimens obtained at necropsy were first homogenized in cell culture medium and then used for virus titration. Virus was measured in biological samples using a standard viral plaque assay and TaqMan q-RT-PCR as described previously (20).

Flow cytometry. Antibodies (with clone designations in parentheses) from BD Biosciences were used for flow cytometry as follows: CD45 (D058-1283), CD3 (SP34-2), CD20 (2H7), CD11c (S-HCL-3), CD123 (7G3), CD14 (M5E2), CD4 (SK3), CD8 (RPA-T8), HLA-DR (L243), active caspase-3 (C92-605), and Ki-67 (B56). Cell viability was assessed using a Live/Dead viability kit (Invitrogen; Carlsbad, CA). All samples were run on a FACSAria II flow cytometer (BD Biosciences) located within the BSL-3 facility.

Statistics. Statistical analyses were performed using GraphPad Prism (La Jolla, CA) software. Statistical tests included two-way analysis of variance (ANOVA), the Mann-Whitney U test, and the *t* test. Probit (dose effect) analysis was conducted using XLSTAT (Addinsoft, New York, NY).

ACKNOWLEDGMENTS

We recognize Tim Sturgeon for flow cytometric expertise and services while inside BSL-3 containment. We also thank Jacquelyn Bales, Laura Bethel, Diana Powell, and Le'Kneitah Smith for technical assistance.

This work was supported by Transformational Medical Technologies program contract HDTRA1-10-C-1066 to A.L.H. from the Department of Defense Chemical and Biological Defense program through the Defense Threat Reduction Agency (DTRA). The funders had no role in study design, data collection and interpretation, or the decision to submit the work for publication.

REFERENCES

1. World Health Organization. 2017. 2017 annual review of diseases prioritized under the Research and Development Blueprint. Informal consultation, 24 to 25 January 2017, Geneva, Switzerland. http://www.who.int/blueprint/what/research-development/2017-Prioritization-Long-Report.pdf?ua=1.
2. Rich KM, Wanyoike F. 2010. An assessment of the regional and national socio-economic impacts of the 2007 Rift Valley fever outbreak in Kenya. Am J Trop Med Hyg 83:52–57. https://doi.org/10.4269/ajtmh.2010.09-0291.
3. Chevalier V, Pépin M, Plée L, Lancelot R. 2010. Rift Valley fever—a threat for Europe? Euro Surveill 15(10):pii=19506. http://www.eurosurveillance.org/content/10.2807/ese.15.10.19506-en.
4. Hartley DM, Rinderknecht JL, Nipp TL, Clarke NP, Snowder GD, National Center for Foreign Animal and Zoonotic Disease Defense Advisory Group on Rift Valley Fever. 2011. Potential effects of Rift Valley fever in the United States. Emerg Infect Dis 17(8):e1. https://doi.org/10.3201/eid1708.101088.
5. Laughlin LW, Meegan JM, Strausbaugh LJ, Morens DM, Watten RH. 1979. Epidemic Rift Valley fever in Egypt: observations of the spectrum of human illness. Trans R Soc Trop Med Hyg 73:630–633. https://doi.org/10.1016/0035-9203(79)90006-3.
6. Madani TA, Al-Mazrou YY, Al-Jeffri MH, Mishkhas AA, Al-Rabeah AM, Turkistani AM, Al-Sayed MO, Abodahish AA, Khan AS, Ksiazek TG, Shobokshi O. 2003. Rift Valley fever epidemic in Saudi Arabia: epidemiological, clinical, and laboratory characteristics. Clin Infect Dis 37:1084–1092. https://doi.org/10.1086/378747.
7. McIntosh BM, Russell D, dos Santos I, Gear JH. 1980. Rift Valley fever in humans in South Africa. S Afr Med J 58:803–806.
8. Mohamed M, Mosha F, Mghamba J, Zaki SR, Shieh WJ, Paweska J, Omulo S, Gikundi S, Mmbuji P, Bloland P, Zeidner N, Kalinga R, Breiman RF, Njenga MK. 2010. Epidemiologic and clinical aspects of a Rift Valley fever outbreak in humans in Tanzania, 2007. Am J Trop Med Hyg 83:22–27. https://doi.org/10.4269/ajtmh.2010.09-0318.
9. van Velden DJ, Meyer JD, Olivier J, Gear JH, McIntosh B. 1977. Rift Valley fever affecting humans in South Africa: a clinicopathological study. S Afr Med J 51:867–871.
10. Al-Hazmi M, Ayoola EA, Abdurahman M, Banzal S, Ashraf J, El-Bushra A, Hazmi A, Abdullah M, Abbo H, Elamin El-Tayeb Al-Sammani A, Gadour TM, Menon C, Hamza M, Rahim I, Hafez M, Jambavalikar M, Arishi H, Aqeel A. 2003. Epidemic Rift Valley fever in Saudi Arabia: a clinical study of severe illness in humans. Clin Infect Dis 36:245–252. https://doi.org/10.1086/345671.
11. Hoogstraal H, Meegan JM, Khalil GM, Adham FK. 1979. The Rift Valley fever epizootic in Egypt 1977–78. 2. Ecological and entomological studies. Trans R Soc Trop Med Hyg 73:624–629. https://doi.org/10.1016/0035-9203(79)90005-1.
12. Gear J, De Meillon B, Measroch V, Davis DH, Harwin H. 1951. Rift valley fever in South Africa. 2. The occurrence of human cases in the Orange Free State, the North-Western Cape Province, the Western and Southern Transvaal. B. Field and laboratory investigation. S Afr Med J 25:908–912.
13. Findlay GM. 1932. Rift Valley Fever or enzootic hepatitis. Trans R Soc Trop Med Hyg 25:229–262. https://doi.org/10.1016/S0035-9203(32)90042-X.
14. Anyangu AS, Gould LH, Sharif SK, Nguku PM, Omolo JO, Mutonga D, Rao CY, Lederman ER, Schnabel D, Paweska JT, Katz M, Hightower A, Njenga MK, Feikin DR, Breiman RF. 2010. Risk factors for severe Rift Valley fever infection in Kenya, 2007. Am J Trop Med Hyg 83:14–21. https://doi.org/10.4269/ajtmh.2010.09-0293.
15. LaBeaud AD, Pfeil S, Muiruri S, Dahir S, Sutherland LJ, Traylor Z, Gildengorin G, Muchiri EM, Morrill J, Peters CJ, Hise AG, Kazura JW, King CH. 2015. Factors associated with severe human Rift Valley fever in Sangailu, Garissa County, Kenya. PLoS Negl Trop Dis 9:e0003548. https://doi.org/10.1371/journal.pntd.0003548.
16. Chambers PG, Swanepoel R. 1980. Rift Valley fever in abattoir workers. Cent Afr J Med 26:122–126.
17. Bales JM, Powell DS, Bethel LM, Reed DS, Hartman AL. 2012. Choice of inbred rat strain impacts lethality and disease course after respiratory infection with Rift Valley fever virus. Front Cell Infect Microbiol 2:105. https://doi.org/10.3389/fcimb.2012.00105.
18. Hartman AL, Powell DS, Bethel LM, Caroline AL, Schmid RJ, Oury T, Reed DS. 2014. Aerosolized Rift Valley fever virus causes fatal encephalitis in African green monkeys and common marmosets. J Virol 88:2235–2245. https://doi.org/10.1128/JVI.02341-13.
19. Smith DR, Bird BH, Lewis B, Johnston SC, McCarthy S, Keeney A, Botto M, Donnelly G, Shamblin J, Albarino CG, Nichol ST, Hensley LE. 2012. Development of a novel nonhuman primate model for Rift Valley fever. J Virol 86:2109–2120. https://doi.org/10.1128/JVI.06190-11.
20. Caroline AL, Kujawa MR, Oury TD, Reed DS, Hartman AL. 2015. Inflam-

matory biomarkers associated with lethal Rift Valley fever encephalitis in the Lewis rat model. Front Microbiol 6:1509. https://doi.org/10.3389/fmicb.2015.01509.
21. Daubney R, Hudson JR. 1933. Rift Valley fever. East Afr Med J 10:2–19.
22. Easterday BC. 1965. Rift Valley fever. Adv Vet Sci 10:65–126.
23. Peters CJ, Jones D, Trotter R, Donaldson J, White J, Stephen E, Slone TW, Jr. 1988. Experimental Rift Valley fever in rhesus macaques. Arch Virol 99:31–44. https://doi.org/10.1007/BF01311021.
24. Morrill JC, Jennings GB, Johnson AJ, Cosgriff TM, Gibbs PH, Peters CJ. 1990. Pathogenesis of Rift Valley fever in rhesus monkeys: role of interferon response. Arch Virol 110:195–212. https://doi.org/10.1007/BF01311288.
25. Cosgriff TM, Morrill JC, Jennings GB, Hodgson LA, Slayter MV, Gibbs PH, Peters CJ. 1989. Hemostatic derangement produced by Rift Valley fever virus in rhesus monkeys. Rev Infect Dis 11(Suppl 4):S807–S814. https://doi.org/10.1093/clinids/11.Supplement_4.S807.
26. Morrill JC, Peters CJ. 2003. Pathogenicity and neurovirulence of a mutagen-attenuated Rift Valley fever vaccine in rhesus monkeys. Vaccine 21:2994–3002. https://doi.org/10.1016/S0264-410X(03)00131-2.
27. Morrill JC, Peters CJ. 2011. Mucosal immunization of rhesus macaques with Rift Valley Fever MP-12 vaccine. J Infect Dis 204:617–625. https://doi.org/10.1093/infdis/jir354.
28. Morrill JC, Peters CJ. 2011. Protection of MP-12-vaccinated rhesus macaques against parenteral and aerosol challenge with virulent Rift Valley fever virus. J Infect Dis 204:229–236. https://doi.org/10.1093/infdis/jir249.
29. Davies FG, Onyango E. 1978. Rift Valley fever: the role of the vervet monkey as a reservoir or maintenance host for this virus. Trans R Soc Trop Med Hyg 72:213–214. https://doi.org/10.1016/0035-9203(78)90074-3.
30. Matsuoka Y, Suguitan A, Jr, Orandle M, Paskel M, Boonnak K, Gardner DJ, Feldmann F, Feldmann H, Marino M, Jin H, Kemble G, Subbarao K. 2014. African green monkeys recapitulate the clinical experience with replication of live attenuated pandemic influenza virus vaccine candidates. J Virol 88:8139–8152. https://doi.org/10.1128/JVI.00425-14.
31. Smith KM, Nanda K, McCarl V, Spears CJ, Piper A, Ribeiro M, Quiles M, Briggs CM, Thomas GS, Thomas ME, Brown DT, Hernandez R. 2012. Testing of novel dengue virus 2 vaccines in African green monkeys: safety, immunogenicity, and efficacy. Am J Trop Med Hyg 87:743–753. https://doi.org/10.4269/ajtmh.2012.12-0004.
32. Bates JT, Pickens JA, Schuster JE, Johnson M, Tollefson SJ, Williams JV, Davis NL, Johnston RE, Schultz-Darken N, Slaughter JC, Smith-House F, Crowe JE. 2016. Immunogenicity and efficacy of alphavirus-derived replicon vaccines for respiratory syncytial virus and human metapneumovirus in nonhuman primates. Vaccine 34:950–956. https://doi.org/10.1016/j.vaccine.2015.12.045.
33. Wang D, Phan S, DiStefano DJ, Citron MP, Callahan CL, Indrawati L, Dubey SA, Heidecker GJ, Govindarajan D, Liang X, He B, Espeseth AS. 2017. A single-dose recombinant parainfluenza virus 5-vectored vaccine expressing respiratory syncytial virus (RSV) F or G protein protected cotton rats and African green monkeys from RSV challenge. J Virol 91:e00066-17. https://doi.org/10.1128/JVI.00066-17.
34. Layton RC, Brasel T, Gigliotti A, Barr E, Storch S, Myers L, Hobbs C, Koster F. 2011. Primary pneumonic plague in the African green monkey as a model for treatment efficacy evaluation. J Med Primatol 40:6–17. https://doi.org/10.1111/j.1600-0684.2010.00443.x.
35. Francis T, Magill TP. 1935. Rift Valley fever: a report of three cases of laboratory infection and the experimental transmission of the disease to ferrets. J Exp Med 62:433–448. https://doi.org/10.1084/jem.62.3.433.
36. Alves DA, Honko AN, Kortepeter MG, Sun M, Johnson JC, Lugo-Roman LA, Hensley LE. 2016. Necrotizing scleritis, conjunctivitis, and other pathologic findings in the left eye and brain of an Ebola virus-infected rhesus macaque (Macaca mulatta) with apparent recovery and a delayed time of death. J Infect Dis 213:57–60. https://doi.org/10.1093/infdis/jiv357.
37. MacIntyre CR, Chughtai AA. 2016. Recurrence and reinfection—a new paradigm for the management of Ebola virus disease. Int J Infect Dis 43:58–61. https://doi.org/10.1016/j.ijid.2015.12.011.
38. Shea MK, Clay KA, Craig DG, Moore AJ, Lewis S, Espina M, Praught J, Horne S, Kao R, Johnston AM. 2016. A health care worker with Ebola virus disease and adverse prognostic factors treated in Sierra Leone. Am J Trop Med Hyg 94:829–832. https://doi.org/10.4269/ajtmh.15-0461.
39. Hunt L, Gupta-Wright A, Simms V, Tamba F, Knott V, Tamba K, Heisenberg-Mansaray S, Tamba E, Sheriff A, Conteh S, Smith T, Tobin S, Brooks T, Houlihan C, Cummings R, Fletcher T. 2015. Clinical presentation, biochemical, and haematological parameters and their association with outcome in patients with Ebola virus disease: an observational cohort study. Lancet Infect Dis 15:1292–1299. https://doi.org/10.1016/S1473-3099(15)00144-9.
40. Akinci E, Bodur H, Sunbul M, Leblebicioglu H. 2016. Prognostic factors, pathophysiology and novel biomarkers in Crimean-Congo hemorrhagic fever. Antiviral Res 132:233–243. https://doi.org/10.1016/j.antiviral.2016.06.011.
41. McElroy AK, Nichol ST. 2012. Rift Valley fever virus inhibits a pro-inflammatory response in experimentally infected human monocyte derived macrophages and a pro-inflammatory cytokine response may be associated with patient survival during natural infection. Virology 422:6–12. https://doi.org/10.1016/j.virol.2011.09.023.
42. Jansen van Vuren P, Shalekoff S, Grobbelaar AA, Archer BN, Thomas J, Tiemessen CT, Paweska JT. 2015. Serum levels of inflammatory cytokines in Rift Valley fever patients are indicative of severe disease. Virol J 12:159. https://doi.org/10.1186/s12985-015-0392-3.
43. Reed DS, Lind CM, Sullivan LJ, Pratt WD, Parker MD. 2004. Aerosol infection of cynomolgus macaques with enzootic strains of Venezuelan equine encephalitis viruses. J Infect Dis 189:1013–1017. https://doi.org/10.1086/382281.
44. Reed DS, Larsen T, Sullivan LJ, Lind CM, Lackemeyer MG, Pratt WD, Parker MD. 2005. Aerosol exposure to western equine encephalitis virus causes fever and encephalitis in cynomolgus macaques. J Infect Dis 192:1173–1182. https://doi.org/10.1086/444397.
45. Reed DS, Lackemeyer MG, Garza NL, Norris S, Gamble S, Sullivan LJ, Lind CM, Raymond JL. 2007. Severe encephalitis in cynomolgus macaques exposed to aerosolized Eastern equine encephalitis virus. J Infect Dis 196:441–450. https://doi.org/10.1086/519391.
46. Porter AI, Erwin-Cohen RA, Twenhafel N, Chance T, Yee SB, Kern SJ, Norwood D, Hartman LJ, Parker MD, Glass PJ, DaSilva L. 2017. Characterization and pathogenesis of aerosolized eastern equine encephalitis in the common marmoset (Callithrix jacchus). Virol J 14:1–15. https://doi.org/10.1186/s12985-016-0669-1.
47. Chaturvedi UC, Mathur A, Tandon P, Natu SM, Rajvanshi S, Tandon HO. 1979. Variable effect on peripheral blood leucocytes during JE virus infection of man. Clin Exp Immunol 38:492–498.
48. Johnson RT, Burke DS, Elwell M, Leake CJ, Nisalak A, Hoke CH, Lorsomrudee W. 1985. Japanese encephalitis: immunocytochemical studies of viral antigen and inflammatory cells in fatal cases. Ann Neurol 18:567–573. https://doi.org/10.1002/ana.410180510.
49. Jaijakul S, Salazar L, Wootton SH, Aguilera E, Hasbun R. 2017. The clinical significance of neutrophilic pleocytosis in cerebrospinal fluid in patients with viral central nervous system infections. Int J Infect Dis 59:77–81. https://doi.org/10.1016/j.ijid.2017.04.010.
50. Dodd KA, McElroy AK, Jones TL, Zaki SR, Nichol ST, Spiropoulou CF. 2014. Rift Valley fever virus encephalitis is associated with an ineffective systemic immune response and activated T cell infiltration into the CNS in an immunocompetent mouse model. PLoS Negl Trop Dis 8:e2874. https://doi.org/10.1371/journal.pntd.0002874.
51. Lathan R, Simon-Chazottes D, Jouvion G, Godon O, Malissen M, Flamand M, Bruhns P, Panthier JJ. 2017. Innate immune basis for Rift Valley fever susceptibility in mouse models. Sci Rep 7:7543. https://doi.org/10.1038/s41598-017-08024-8.
52. Jansen van Vuren P, Tiemessen CT, Paweska JT. 2011. Anti-nucleocapsid protein immune responses counteract pathogenic effects of Rift Valley fever virus infection in mice. PLoS One 6:e25027. https://doi.org/10.1371/journal.pone.0025027.
53. Dodd KA, McElroy AK, Jones ME, Nichol ST, Spiropoulou CF. 2013. Rift Valley fever virus clearance and protection from neurologic disease are dependent on $CD4^+$ T cell and virus-specific antibody responses. J Virol 87:6161–6171. https://doi.org/10.1128/JVI.00337-13.
54. Xu W, Watts DM, Costanzo MC, Tang X, Venegas LA, Jiao F, Sette A, Sidney J, Sewell AK, Wooldridge L, Makino S, Morrill JC, Peters CJ, Kan-Mitchell J. 2013. The nucleocapsid protein of Rift Valley fever virus is a potent human $CD8^+$ T cell antigen and elicits memory responses. PLoS One 8:e59210. https://doi.org/10.1371/journal.pone.0059210.
55. Wallace DB, Ellis CE, Espach A, Smith SJ, Greyling RR, Viljoen GJ. 2006. Protective immune responses induced by different recombinant vaccine regimes to Rift Valley fever. Vaccine 24:7181–7189. https://doi.org/10.1016/j.vaccine.2006.06.041.
56. Papa A, Tsergouli K, Çağlayik DY, Bino S, Como N, Uyar Y, Korukluoglu G.

2016. Cytokines as biomarkers of Crimean-Congo hemorrhagic fever. J Med Virol 88:21–27. https://doi.org/10.1002/jmv.24312.
57. McElroy AK, Erickson BR, Flietstra TD, Rollin PE, Nichol ST, Towner JS, Spiropoulou CF. 2014. Ebola hemorrhagic fever: novel biomarker correlates of clinical outcome. J Infect Dis 210:558–566. https://doi.org/10.1093/infdis/jiu088.
58. do Valle TZ, Billecocq A, Guillemot L, Alberts R, Gommet C, Geffers R, Calabrese K, Schughart K, Bouloy M, Montagutelli X, Panthier JJ. 2010. A new mouse model reveals a critical role for host innate immunity in resistance to Rift Valley fever. J Immunol 185:6146–6156. https://doi.org/10.4049/jimmunol.1000949.
59. Billecocq A, Spiegel M, Vialat P, Kohl A, Weber F, Bouloy M, Haller O. 2004. NSs protein of Rift Valley fever virus blocks interferon production by inhibiting host gene transcription. J Virol 78:9798–9806. https://doi.org/10.1128/JVI.78.18.9798-9806.2004.
60. Bouloy M, Janzen C, Vialat P, Khun H, Pavlovic J, Huerre M, Haller O. 2001. Genetic evidence for an interferon-antagonistic function of Rift Valley fever virus nonstructural protein NSs. J Virol 75:1371–1377. https://doi.org/10.1128/JVI.75.3.1371-1377.2001.
61. Ikegami T, Narayanan K, Won S, Kamitani W, Peters CJ, Makino S. 2009. Dual functions of Rift Valley fever virus NSs protein: inhibition of host mRNA transcription and post-transcriptional downregulation of protein kinase PKR. Ann N Y Acad Sci 1171(Suppl 1):E75–E85. https://doi.org/10.1111/j.1749-6632.2009.05054.x.
62. Hise AG, Traylor Z, Hall NB, Sutherland LJ, Dahir S, Ermler ME, Muiruri S, Muchiri EM, Kazura JW, LaBeaud AD, King CH, Stein CM. 2015. Association of symptoms and severity of Rift Valley fever with genetic polymorphisms in human innate immune pathways. PLoS Negl Trop Dis 9:e0003584. https://doi.org/10.1371/journal.pntd.0003584.
63. Tokuda S, Do Valle TZ, Batista L, Simon-Chazottes D, Guillemot L, Bouloy M, Flamand M, Montagutelli X, Panthier JJ. 2015. The genetic basis for susceptibility to Rift Valley fever disease in MBT/Pas mice. Genes Immun 16:206–212. https://doi.org/10.1038/gene.2014.79.
64. National Research Council. 2011. Guide for the care and use of laboratory animals, 8th ed. National Academies Press, Washington, DC.
65. Reed DS, Bethel LM, Powell DS, Caroline AL, Hartman AL. 2014. Differences in aerosolization of Rift Valley fever virus resulting from choice of inhalation exposure chamber: implications for animal challenge studies. Pathog Dis 71:227–233. https://doi.org/10.1111/2049-632X.12157.
66. Roy CJ, Pitt LM. 2005. Infectious disease aerobiology: aerosol challenge methods, p 61–76. *In* Swearengen JR (ed), Biodefense: research methodology and animal models. CRC Press, Boca Raton, FL.
67. Brown KN, Barratt-Boyes SM. 2009. Surface phenotype and rapid quantification of blood dendritic cell subsets in the rhesus macaque. J Med Primatol 38:272–278. https://doi.org/10.1111/j.1600-0684.2009.00353.x.